Science Advances
AAAS

Supplementary Materials for

Multiscale 3D genome reorganization during skeletal muscle stem cell lineage progression and aging

Yu Zhao *et al.*

Corresponding author: Yu Zhao, zhaoyu25@mail.sysu.edu.cn; Hao Sun, haosun@cuhk.edu.hk; Huating Wang, huating.wang@cuhk.edu.hk

Sci. Adv. **9**, eabo1360 (2023)
DOI: 10.1126/sciadv.abo1360

The PDF file includes:

Other Supplementary Material for this manuscript includes the following:

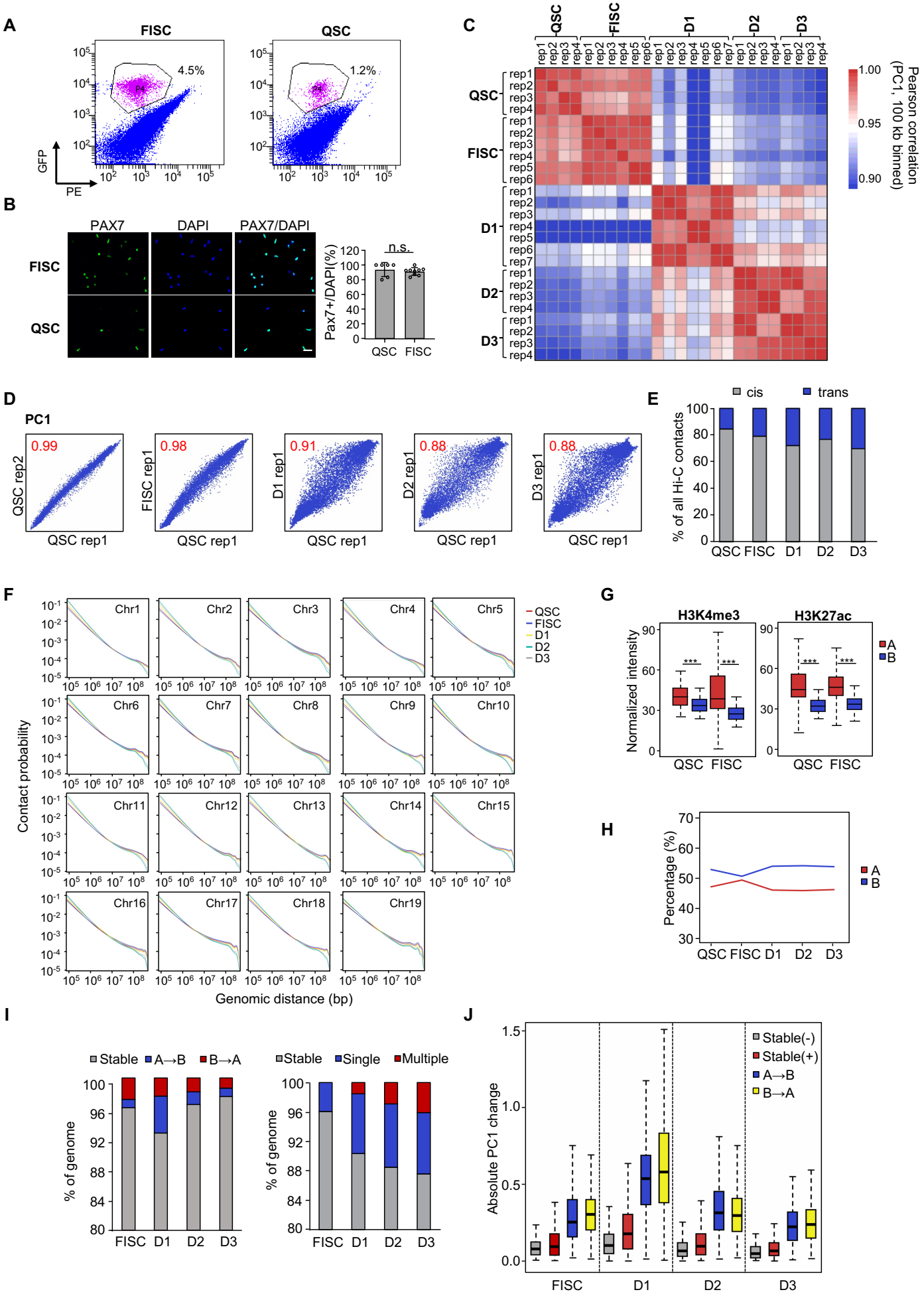
A
FISC
QSC
4.5%
1.2%
GFP
PE
B
PAX7
DAPI
PAX7/DAPI
FISC
QSC
Pax7+/DAPI(%)
n.s.
C
Pearson correlation (PC1, 100 kb binned)
D
PC1
0.99
0.98
0.91
0.88
0.88
QSC rep2
FISC rep1
D1 rep1
D2 rep1
D3 rep1
QSC rep1
E
cis
trans
% of all Hi-C contacts
F
Contact probability
Genomic distance (bp)
G
H3K4me3
H3K27ac
Normalized intensity
H
Percentage (%)
I
Stable
A→B
B→A
Single
Multiple
% of genome
J
Absolute PC1 change
Stable(-)
Stable(+)

Figure S1. Global reorganization of genome compartmentalization during SC lineage development. (A) GFP+ FISCs or QSCs were collected from *Pax7-nGFP* muscle by FACS sorting. FACS profiles are shown. GFP+ cells are marked as magenta dots. Values on the plots indicate mean percentage of sorted GFP+ cells in the total number of events. **(B)** Immunofluorescence staining for PAX7 was performed on the above collected QSC and FISC. The percentage of PAX7+ cells is shown on the right. Scale bar, 10 μm. n = 6-9 fields. **(C)** *In situ* Hi-C was performed on QSC, FISC, ASC-D1, ASC-D2, or DSC-D3. Heat map showing the Pearson correlation among all replicates of Hi-C samples, based on the PC1 values (100 kb bins). **(D)** Scatter plots of PC1 values showing change of each time point relative to QSC replicate 1. Pearson correlation coefficients are indicated. **(E)** The percentage of *cis* and *trans* chromosomal Hi-C contacts in the Hi-C datasets at each time point. **(F)** Contact probability relative to genomic distance of individual chromosomes. **(G)** Enrichment of H3K4me3 and H3K27Ac ChIP-seq signals in A or B compartments in QSC and FISC. ***$P < 0.0001$, Wilcoxon signed-rank test. **(H)** Line chart depicting fraction of the genome assigned to A or B compartments at each time point. **(I)** Left, bar graph depicting fraction of the genome that switched compartment between any two time points. Right, bar graph depicting switching percentage per time point. **(J)** Absolute PC1 change between any two time points for regions that switched compartment (A→B or B→A) or did not switch ('stable') but increased (+) or decreased (-) in PC1 value.

A

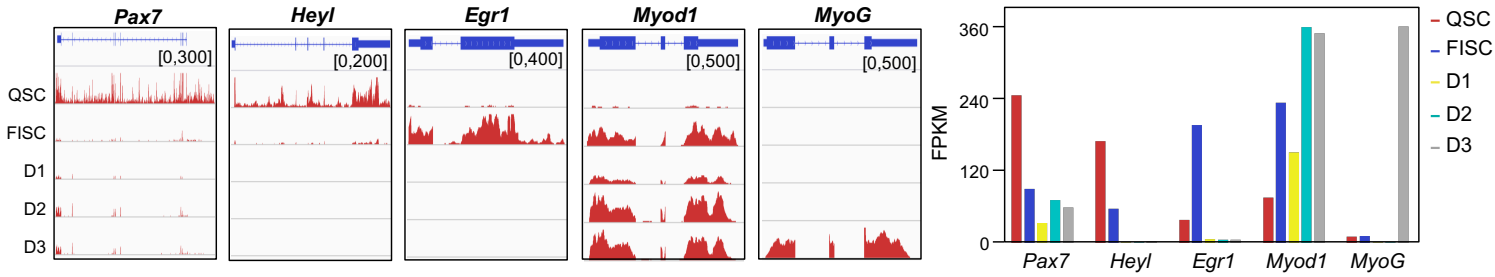

B

RNA/PC1 dynamics:

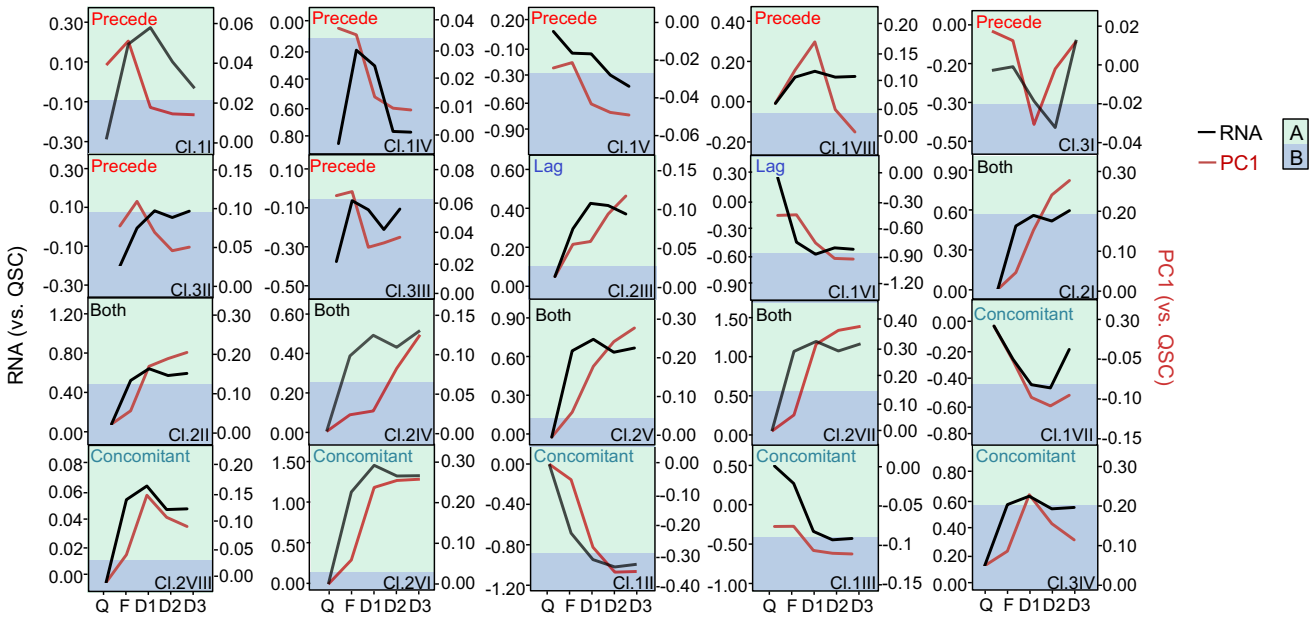

C

B-to-A switch

Cluster	Gene no.	Class	GO term
1I	249	Preceding	negative regulation of DNA demethylation
1II	137	Concomitant	negative regulation of complement activation
1III	199	Concomitant	nucleic acid binding
1IV	282	Preceding	transcription factor complex
1V	295	Preceding	transcription coactivator activity
1VI	201	Lagging	cell division& cell cycle
IVII	98	Concomitant	positive regulation of fibroblast proliferation
1VIII	103	Preceding	nucleic acid binding, cell junction

A-to-B switch

Cluster	Gene no.	Class	GO term
2I	91	Both	cell migration
2II	125	Both	DNA binding
2III	168	Lag	regulation of the apoptotic process
2IV	151	Both	positive regulation of transcription, DNA-templated
2V	202	Both	cell development
2VI	147	Concomitant	extracellular exosome
2VII	82	Both	protein processing
2VIII	103	Concomitant	protein auto phosphorylation

Multiple switch

Cluster	Gene no.	Class	GO term
3I	193	Preceding	positive regulation of transcription from RNA polymerase II promoter
3II	209	Preceding	myofibril
3III	208	Preceding	cell differentiation
3IV	117	Concomitant	cell junction, cell communication

Figure S2. Integrated kinetics of transcriptome and compartmentalization during SC lineage development. (A) left: Genome browser view of *Pax7*, *Heyl*, *Egr1*, *Myod1* and *MyoG* gene expression measured by RNA-seq data; right: bar graph depicting the RPKM values of the above genes across the SC lineage progression. **(B)** 20 types of switching clusters were identified and the dynamics of average RNA expression versus PC1 are shown. **(C)** Summarized gene ontology (GO) annotation of the 20 clusters grouped by switching dynamics during SC lineage progression.

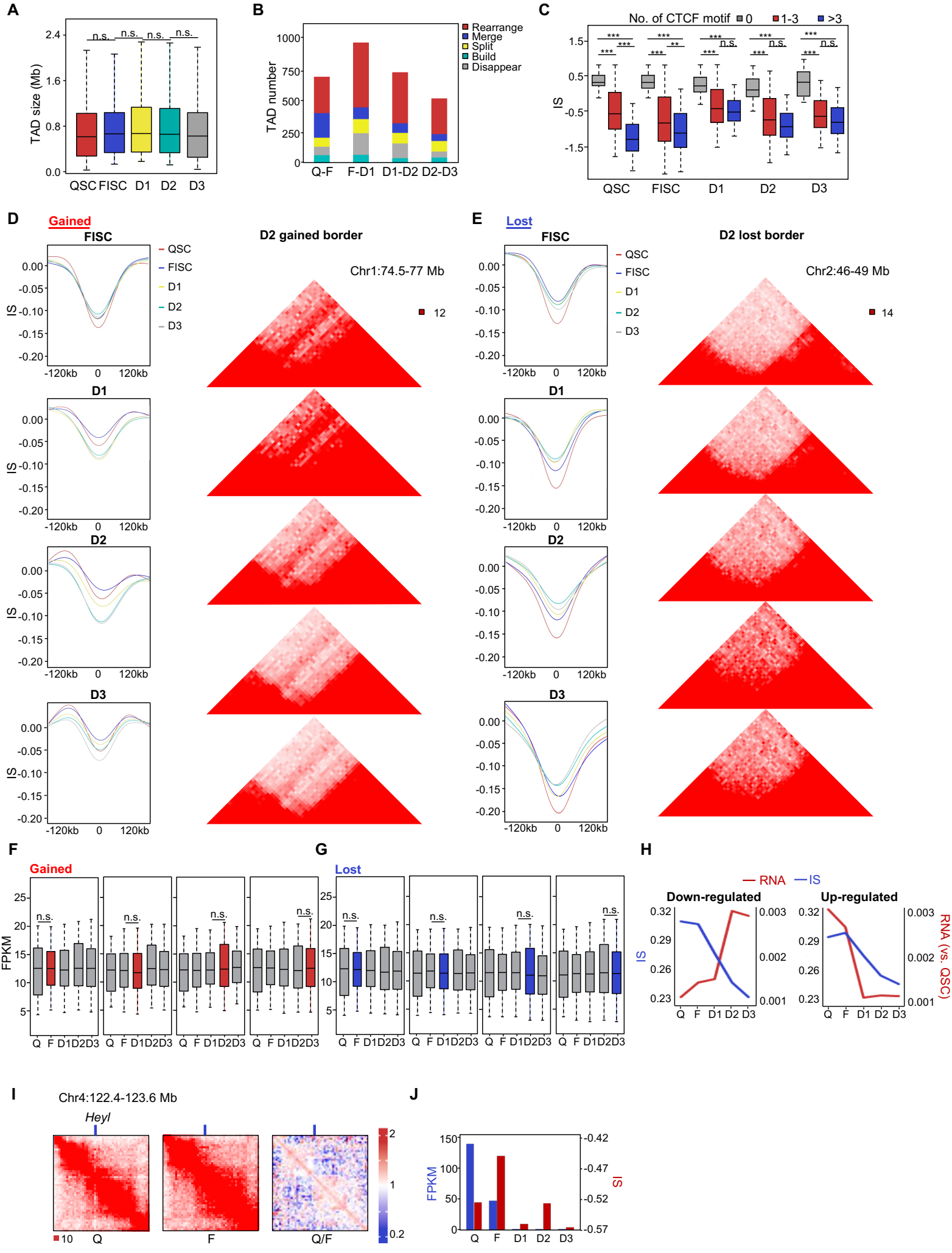
A
TAD size (Mb)
n.s.
QSC FISC D1 D2 D3
B
TAD number
Rearrange
Merge
Split
Build
Disappear
Q-F F-D1 D1-D2 D2-D3
C
No. of CTCF motif 0 1-3 >3
IS
QSC FISC D1 D2 D3
D
Gained
FISC
D1
D2
D3
IS
-120kb 0 120kb
D2 gained border
Chr1:74.5-77 Mb
12
E
Lost
D2 lost border
Chr2:46-49 Mb
14
F
Gained
FPKM
Q F D1 D2 D3
G
Lost
H
RNA IS
Down-regulated
Up-regulated
RNA (vs. QSC)
I
Chr4:122.4-123.6 Mb
Heyl
10
Q F Q/F
J
FPKM
IS

Figure S3. Dynamic TAD boundary organization during SC lineage development. (A) Boxplots showing TAD size distribution at each stage. **(B)** Bar graph showing the number of TADs that were rearranged, merged, split, built or disappeared between two adjacent stages. **(C)** Boxplots showing IS of TAD borders harboring 0, 1-3 or >3 CTCF motifs**. (D-E)** Average IS in a 240 kb region centered on TAD boundaries gained or lost over time during SC lineage progression. Lines show mean values (left). Representative *in situ* Hi-C contact maps of a novel boundary gained at D2 (D, right) or lost at D2 (E, right). **(F-G)** Boxplots depicting gene expression (RPKM) dynamics for border regions that were gained (red) or lost (blue) during SC development. **(H)** Kinetics of mean expression level (FPKM) changes at dynamic borders harboring genes that were either up-regulated or down-regulated after IS decreased. **(I)** Illustration of *in situ* Hi-C contact maps (40-kb resolution) on the *Heyl* locus. **(J)** Bar graph showing IS and FPKM kinetics of *Heyl* residing TAD border. Data in A, C, F, and G are presented in boxplots. $^{**}P < 0.001$, $^{***}P < 0.0001$, n.s., no significance, Wilcoxon signed-rank test.

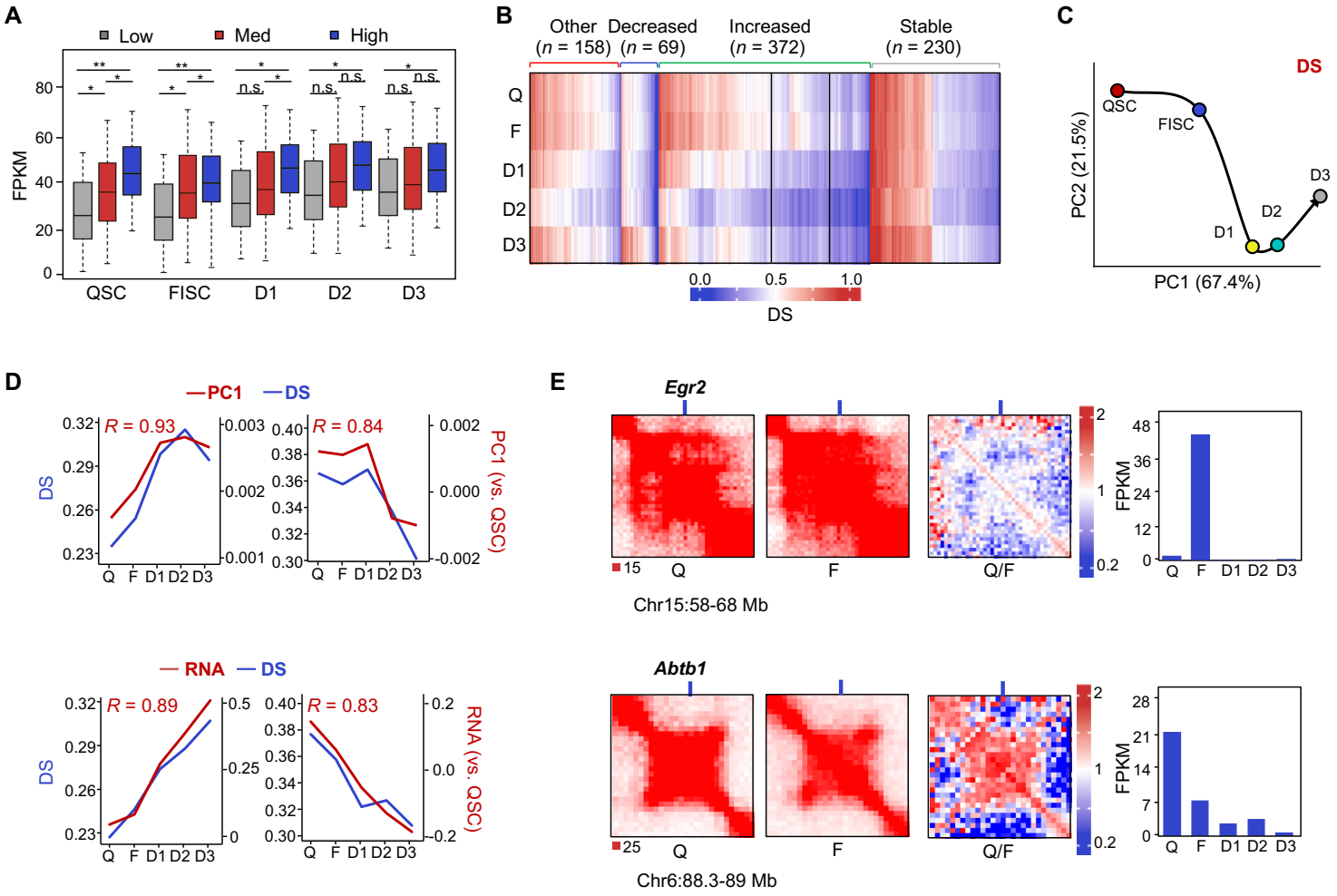
A
Low
Med
High
FPKM
QSC
FISC
D1
D2
D3
B
Other (n = 158)
Decreased (n = 69)
Increased (n = 372)
Stable (n = 230)
Q
F
D1
D2
D3
DS
C
DS
QSC
FISC
D1
D2
D3
PC2 (21.5%)
PC1 (67.4%)
D
PC1
DS
R = 0.93
R = 0.84
PC1 (vs. QSC)
RNA
DS
R = 0.89
R = 0.83
RNA (vs. QSC)
E
Egr2
Chr15:58-68 Mb
Abtb1
Chr6:88.3-89 Mb
Q
F
Q/F
FPKM

Figure S4. Intra-TAD interactions are rewired during SC lineage development. (A) Boxplots depicting average expression of genes (FPKM) in TADs with a low (0, 0.3), med (0.3,0.6) or high (0.6, 1) D-score at each stage. *$P < 0.01$, **$P < 0.001$, n.s., no significance, Wilcoxon signed-rank test. **(B)** *k*-means clustering ($k = 20$) of D scores. **(C)** PCA of D-score during SC lineage progression. Hypothetical trajectory is shown as black arrow. **(D)** Average D-score and PC1 kinetics (top) or gene expression (bottom) analysis for clusters of TADs that were gained ($n = 2{,}172$, left) or lost ($n = 467$, right) in D3 vs QSC. Pearson correlation coefficients (*R*) are indicated. (**E**) Illustration of *in situ* Hi-C contact maps (40-kb resolution) on the *Egr2* locus on Chr15 (top) and on the *Abtb1* locus on Chr6 (bottom). The bar graphs show the FPKM kinetics of *Egr2* and *Abtb1* expression.

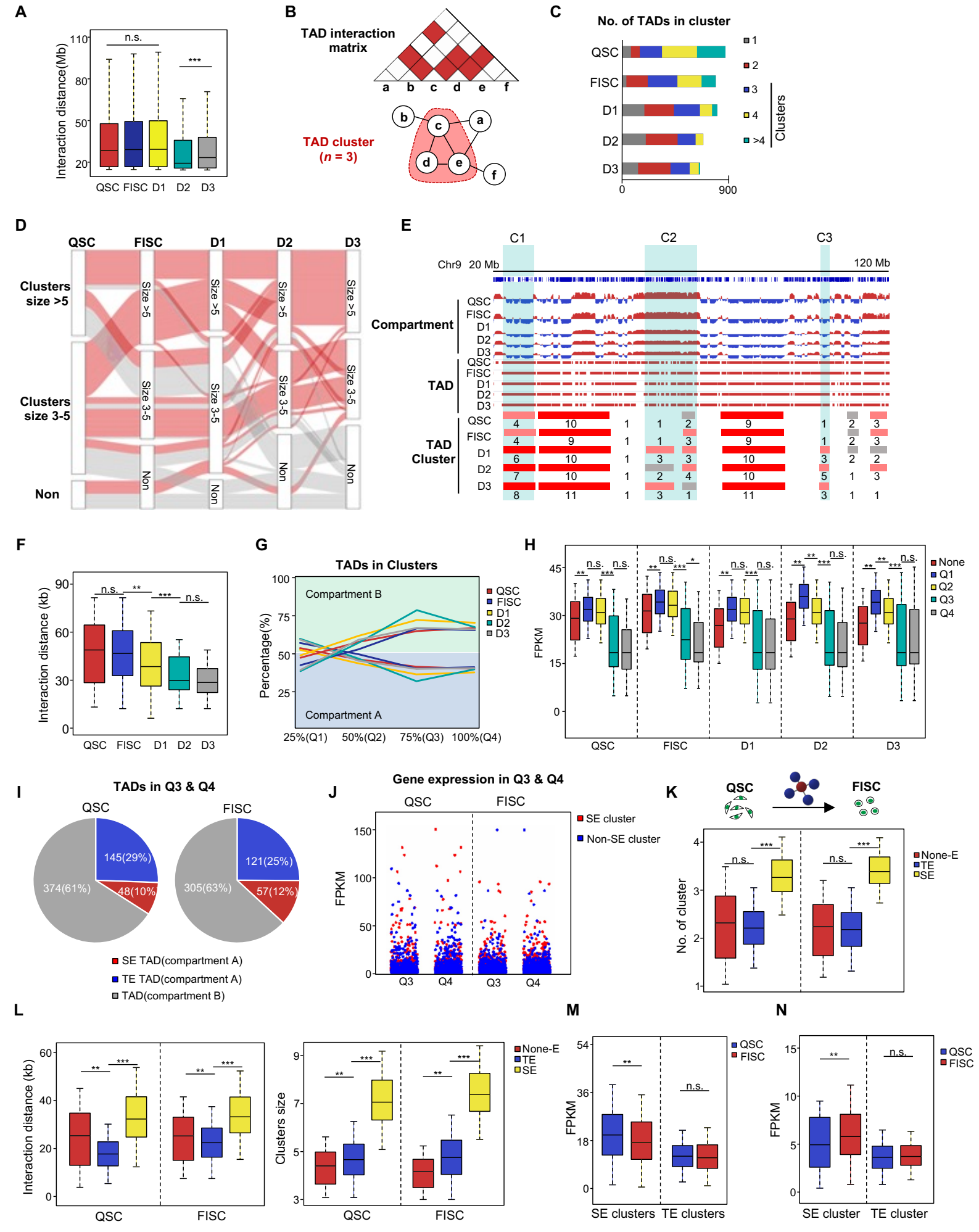
A
Interaction distance(Mb)
110
80
50
20
n.s.
***
QSC FISC D1 D2 D3
B
TAD interaction matrix
a b c d e f
TAD cluster (n = 3)
C
No. of TADs in cluster
QSC
FISC
D1
D2
D3
0
900
1
2
3
4
>4
Clusters
D
QSC FISC D1 D2 D3
Clusters size >5
Clusters size 3-5
Non
Size >5
Size 3-5
Non
E
C1 C2 C3
Chr9 20 Mb
120 Mb
Compartment
TAD
TAD Cluster
QSC
FISC
D1
D2
D3
F
Interaction distance (kb)
90
60
30
0
n.s.
**
***
n.s.
QSC FISC D1 D2 D3
G
TADs in Clusters
Percentage(%)
100
75
50
25
Compartment B
Compartment A
25%(Q1) 50%(Q2) 75%(Q3) 100%(Q4)
QSC
FISC
D1
D2
D3
H
FPKM
45
30
15
0
n.s.
*
**
***
QSC FISC D1 D2 D3
None
Q1
Q2
Q3
Q4
I
TADs in Q3 & Q4
QSC
FISC
145(29%)
48(10%)
374(61%)
121(25%)
57(12%)
305(63%)
SE TAD(compartment A)
TE TAD(compartment A)
TAD(compartment B)
J
Gene expression in Q3 & Q4
QSC
FISC
FPKM
150
100
50
0
Q3 Q4 Q3 Q4
SE cluster
Non-SE cluster
K
QSC
FISC
No. of cluster
4
3
2
1
n.s.
***
None-E
TE
SE
L
Interaction distance (kb)
60
40
20
0
**
***
QSC FISC
Clusters size
9
7
5
3
None-E
TE
SE
M
FPKM
54
36
18
0
**
n.s.
SE clusters TE clusters
QSC
FISC
N
FPKM
15
10
5
0
**
n.s.
SE cluster TE cluster
QSC
FISC

Figure S5. TAD clusters are dynamically reorganized in FISC vs. QSC. (A) Boxplots showing the average distance between pair-wise TAD interactions at each time point. **(B)** (top) illustration of significant interactions between TADs in a matrix (red pixels). (bottom) A TAD cluster (pink) is identified when ⩾3 TADs are fully connected with each other. Edges indicating interaction between two TADs while nodes indicating TADs. **(C)** Bar charts depicting the number of TADs in clusters as a function of cluster size at each time point. **(D)** TAD clusters were defined during SC development. Alluvial representation plot showing the formation, loss, expansion and reduction of TAD clusters. Line thickness is proportional to the number of TADs within the clusters on D3 (line color: red, size >5 or 3-5; gray, non-clusters). **(E)** Genome-browser view of compartment, TAD and TAD cluster of a 100 Mb region on chr 9. The number of TADs in each TAD cluster is shown (bottom tracks). Three dynamic TAD clusters are highlighted in blue box. **(F)** Box plots showing the average distance between pair-wise TAD interactions in TAD clusters at each time point. (**G**) TADs in clusters were stratified by quartile of distances between pair-wise TAD interactions. Line charts depicting the fraction of TADs in clusters of each quartile in A and B compartments over time of SC development. (**H**) Gene expression levels outside clusters (Non) and in clusters of each quartile (Q1, Q2, Q3 or Q4) over time of SC development. **(I)** TADs are classified into four quartiles (Q1, Q2, Q3 and Q4) according to distance between pair-wise interacting TADs. Pie chart showing the distribution of SE/TE containing TADs in Q3 and Q4. **(J)** Expression of genes residing in pair-wise interacting TADs in Q3 and Q4. Blue, genes in SE containing TAD clusters; Red, genes in TAD clusters without SE. **(K)** Boxplots showing the relative number of TAD clusters engaging TE, SE or random control regions at QSC or FISC stage. **(L)** Left, Boxplots showing the average distance between pair-wise TAD interactions that TE or SE engaged in at QSC or FISC stage. Right, Boxplots showing the size of TAD clusters (i.e. the number of TADs within a TAD cluster) engaging TE, SE or random control regions at QSC or FISC stage. **(M-N)** Boxplots depicting expression dynamics (RPKM) in FISC vs. QSC for TAD clusters with TE or SE engagement at QSC (M) or FISC (N) stage. Data in A, F, H, K, L, M and N are presented in boxplots. *$P < 0.01$, **$P < 0.001$, ***$P < 0.0001$. n.s., no significance, Wilcoxon signed-rank test.

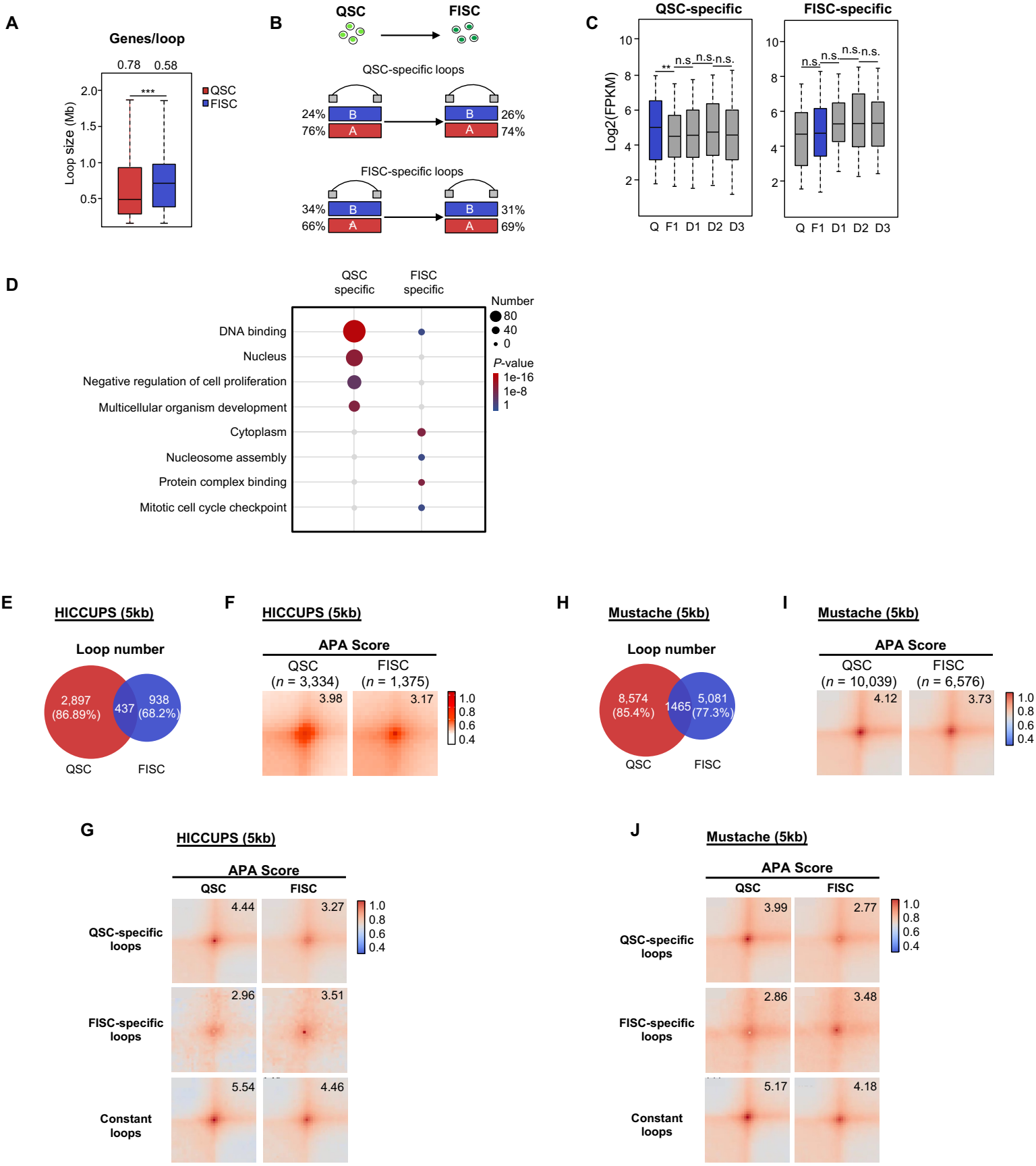
A
Genes/loop
0.78
0.58
***
QSC
FISC
Loop size (Mb)
2.0
1.5
1.0
0.5
B
QSC
FISC
QSC-specific loops
24%
76%
B
A
26%
74%
FISC-specific loops
34%
66%
31%
69%
C
QSC-specific
FISC-specific
Log2(FPKM)
**
n.s.
Q F1 D1 D2 D3
D
QSC specific
FISC specific
Number
80
40
0
P-value
1e-16
1e-8
1
DNA binding
Nucleus
Negative regulation of cell proliferation
Multicellular organism development
Cytoplasm
Nucleosome assembly
Protein complex binding
Mitotic cell cycle checkpoint
E
HICCUPS (5kb)
Loop number
2,897
(86.89%)
437
938
(68.2%)
QSC
FISC
F
HICCUPS (5kb)
APA Score
QSC
(n = 3,334)
FISC
(n = 1,375)
3.98
3.17
1.0
0.8
0.6
0.4
G
HICCUPS (5kb)
APA Score
QSC
FISC
QSC-specific loops
4.44
3.27
FISC-specific loops
2.96
3.51
Constant loops
5.54
4.46
H
Mustache (5kb)
Loop number
8,574
(85.4%)
1465
5,081
(77.3%)
QSC
FISC
I
Mustache (5kb)
APA Score
QSC
(n = 10,039)
FISC
(n = 6,576)
4.12
3.73
J
Mustache (5kb)
APA Score
QSC
FISC
QSC-specific loops
3.99
2.77
FISC-specific loops
2.86
3.48
Constant loops
5.17
4.18

Figure S6. Chromatin loops are dynamically rewired during SC early activation. (A) Boxplot depicting loop size in QSC and FISC. Average number of genes per loop in QSC and FISC are show above. **(B)** Illustration showing the percentage of QSC- or FISC- specific loops within A or B compartments. **(C)** Box plot depicting expression dynamics of genes within QSC- or FISC- specific loops. **(D)** Bubble plot of the enriched GO terms associated with genes in QSC- or FISC- specific loops. The bubble size represents the number of genes enriched in each term; the bubble color represents the enrichment significance. **(E)** Pie chart showing the overlapping between chromatin loops detected in QSC (n = 3,334) and FISC (n = 1,375) by HICCUPS. **(F)** Aggregated peak analysis (APA) analysis of all chromatin loops detected by HICCUPS at QSC or FISC. Bin size, 5 kb. **(G)** APA analysis of QSC- or FISC-specific loops and constant loops detected by HICCUPS. Bin size, 5 kb. Numbers indicate average loop strength. **(H-J)** The above chromatin loop analyses were conducted by Mustache. Data in A and C are presented in boxplots. $^{**}P < 0.001$, $^{***}P < 0.0001$. n.s., no significance, Wilcoxon signed-rank test.

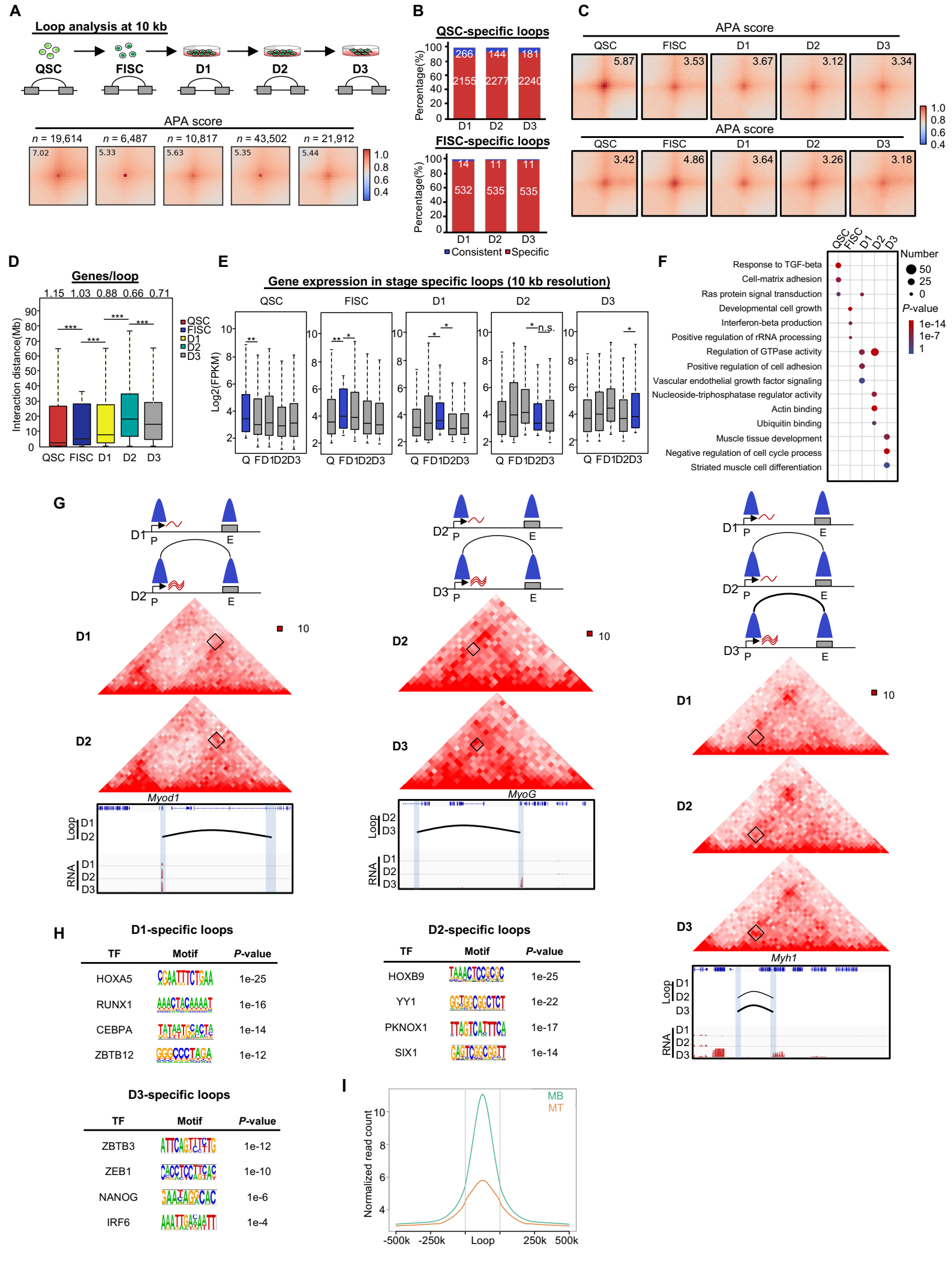
A
Loop analysis at 10 kb
QSC
FISC
D1
D2
D3
APA score
n = 19,614
n = 6,487
n = 10,817
n = 43,502
n = 21,912
7.02
5.33
5.63
5.35
5.44
1.0
0.8
0.6
0.4
B
QSC-specific loops
Percentage(%)
266
144
181
2155
2277
2240
D1
D2
D3
FISC-specific loops
14
11
11
532
535
535
Consistent
Specific
C
APA score
QSC
FISC
D1
D2
D3
5.87
3.53
3.67
3.12
3.34
3.42
4.86
3.64
3.26
3.18
D
Genes/loop
1.15 1.03 0.88 0.66 0.71
Interaction distance(Mb)
E
Gene expression in stage specific loops (10 kb resolution)
Log2(FPKM)
n.s.
F
Number
50
25
0
P-value
1e-14
1e-7
1
Response to TGF-beta
Cell-matrix adhesion
Ras protein signal transduction
Developmental cell growth
Interferon-beta production
Positive regulation of rRNA processing
Regulation of GTPase activity
Positive regulation of cell adhesion
Vascular endothelial growth factor signaling
Nucleoside-triphosphatase regulator activity
Actin binding
Ubiquitin binding
Muscle tissue development
Negative regulation of cell cycle process
Striated muscle cell differentiation
G
P
E
Myod1
MyoG
Myh1
Loop
RNA
H
D1-specific loops
TF
Motif
P-value
HOXA5
1e-25
RUNX1
1e-16
CEBPA
1e-14
ZBTB12
1e-12
D2-specific loops
HOXB9
1e-25
YY1
1e-22
PKNOX1
1e-17
SIX1
1e-14
D3-specific loops
ZBTB3
1e-12
ZEB1
1e-10
NANOG
1e-6
IRF6
1e-4
I
Normalized read count
MB
MT
-500k
-250k
Loop
250k
500k

Figure S7. Dynamics of chromatin loops during SC lineage progression. (A) (top) Illustration of identified chromatin loops in QSC, FISC, D1, D2 and D3. Bin size, 10 kb. (Bottom) Aggregated peak analysis (APA) analysis of all chromatin loops detected at QSC (*n* = 19,614), FISC (*n* = 6,487), D1 (*n* = 10,817), D2 (*n* = 43,502) and D3 (*n* = 21,912). Bin size, 10 kb. **(B)** Bar graph depicting the number and fraction of QSC-specific loops (top) and FISC-specific loops (bottom) that appeared at the late stages. **(C)** Aggregated peak analysis (APA) analysis of QSC-specific loops or FISC-specific loops at each time point. Bin size, 10 kb. **(D)** Boxplot depicting changes in loop size during SC lineage progression. Average number of genes per loop are show above. **(E)** Box plot depicting expression dynamics of genes within stage–specific loops. **(F)** Bubble plot of the enriched GO terms associated with genes in stage-specific loops. The bubble size represents the number of genes enriched in each term; the bubble color represents the enrichment significance. **(G)** Hi-C contact maps depicting stage-specific loops form around *Myod1*, *MyoG*, and *Myh1* genomic locus during SC lineage progression. Left, black square in Hi-C contact matrix and black arc denote a chromatin loop formed between *Myod1* locus and a downstream region at D2. RNA-seq tracks showing the induction of *Myod1* RNA expression at D2. Middle, black square in Hi-C contact matrix and black arc denote a chromatin loop formed between *MyoG* locus and an upstream region at D3. RNA-seq tracks showing the induction of *MyoG* RNA expression at D3. Right, black square in Hi-C contact matrix and black arc denote a chromatin loop formed between *Myh1* locus and an upstream region at D2 and strengthened at D3. RNA-seq tracks showing the induction of *Myh1* RNA expression at D3. **(H)** Motif enrichment was conducted in the stage-specific loop anchors by HOMER. **(I)** YY1 ChIP-seq profiles in myoblast (MB) or myotube (MT) were collected. Meta plot showing the enrichment of YY1 occupancy in the anchors of D2-specific loops (YY1 ChIP-seq in MB) and reduced enrichment of YY1 binding in D3-specific loop anchors (YY1 ChIP-seq in MT). Data in D and E are presented in boxplots. **P* < 0.01, ***P* < 0.001, ****P* < 0.0001. n.s., no significance, Wilcoxon signed-rank test.

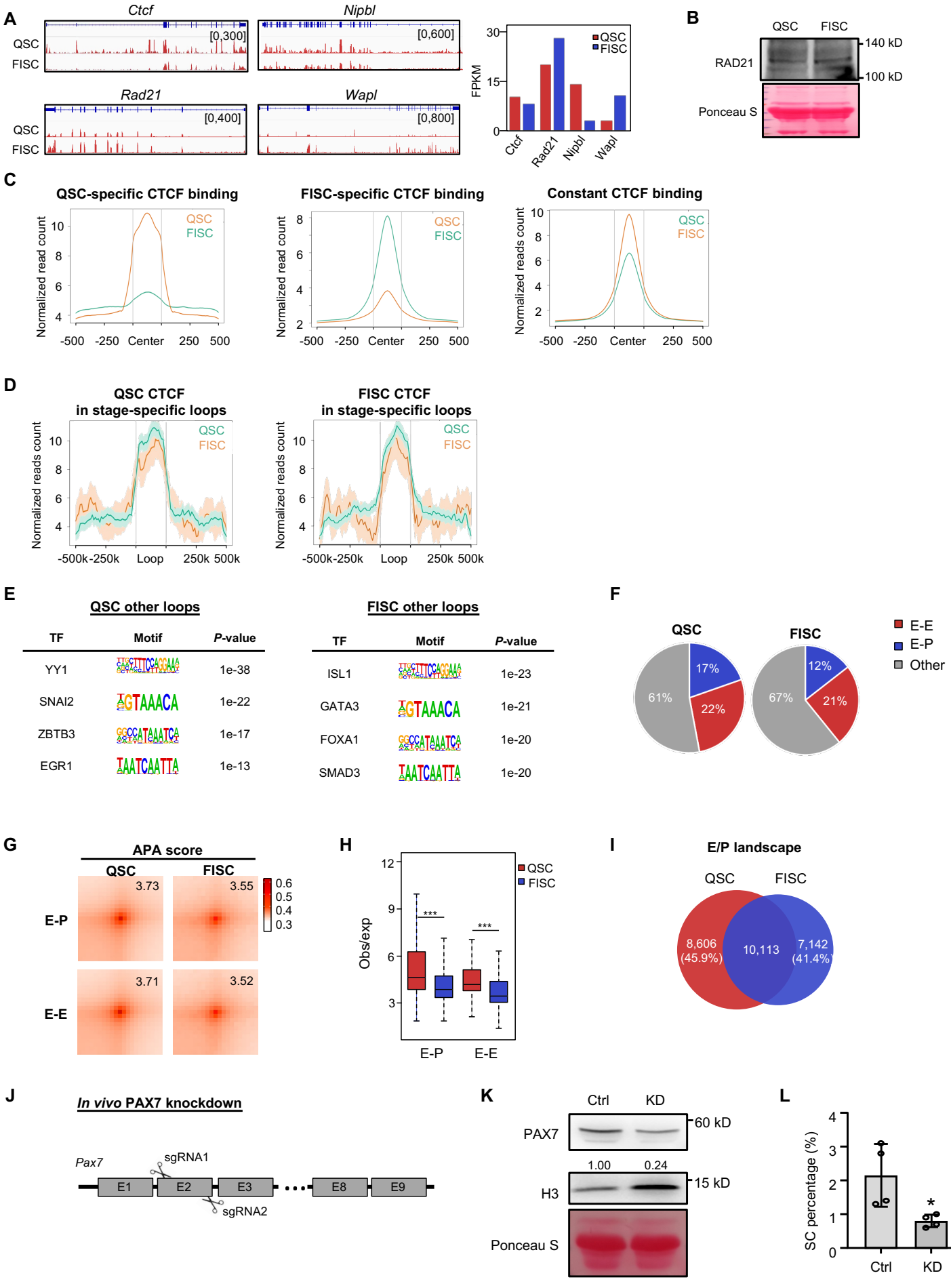
A
Ctcf
Nipbl
Rad21
Wapl
QSC
FISC
[0,300]
[0,600]
[0,400]
[0,800]
FPKM
30
15
0
Ctcf
Rad21
Nipbl
Wapl
B
QSC
FISC
RAD21
Ponceau S
140 kD
100 kD
C
QSC-specific CTCF binding
FISC-specific CTCF binding
Constant CTCF binding
Normalized read count
Normalized reads count
-500
-250
Center
250
500
D
QSC CTCF
in stage-specific loops
FISC CTCF
in stage-specific loops
-500k
-250k
Loop
250k
500k
E
QSC other loops
FISC other loops
TF
Motif
P-value
YY1
1e-38
SNAI2
1e-22
ZBTB3
1e-17
EGR1
1e-13
ISL1
1e-23
GATA3
1e-21
FOXA1
1e-20
SMAD3
1e-20
F
QSC
FISC
17%
22%
61%
12%
21%
67%
E-E
E-P
Other
G
APA score
QSC
FISC
E-P
E-E
3.73
3.55
3.71
3.52
0.6
0.5
0.4
0.3
H
Obs/exp
***
E-P
E-E
I
E/P landscape
8,606
(45.9%)
10,113
7,142
(41.4%)
J
In vivo PAX7 knockdown
Pax7
sgRNA1
sgRNA2
E1
E2
E3
E8
E9
K
Ctrl
KD
PAX7
H3
Ponceau S
60 kD
15 kD
1.00
0.24
L
SC percentage (%)
*
Ctrl
KD

Figure S8. PAX7 regulates E/P loop reorganization during SC early activation. (A) Left: RNA-seq tracks showing *Ctcf*, *Rad21*, *Nipbl* and *Wapl* mRNA expression in QSC and FISC. Right: bar graphs showing the RNA expression levels (FPKM). **(B)** Western blot analysis of RAD21 protein in QSC and FISC. Ponceau S staining was used as loading control. **(C)** CTCF ChIP-seq binding peaks in QSC and FISC were analyzed. QSC-specific, FISC-specific and constant binding peaks were identified and Meta plot showing the CTCF binding signals in each category. **(D)** Enriched CTCF binding signals at the anchor regions of QSC- or FISC-specific loops. **(E)** Enriched TF motifs in the loop anchors of "other" loops in QSC and FISC conducted by HOMER. **(F)** Distribution of enhancer-enhancer (E-E), Enhancer-Promoter (E-P) and other types of loops among E/P loops in QSC and FISC. **(G)** APA analysis of E-E and E-P chromatin loops detected in QSC and FISC. **(H)** Box plot depicting interaction intensity (Obs/exp) of the above E-E and E-P loops. ***$P < 0.0001$, Wilcoxon signed-rank test. **(I)** Overlapping of active enhancers and promoters between QSC and FISC. The number and the percentage of overlapped and specific enhancers and promoters are shown. **(J)** Schematic illustration showing the design of dual sgRNAs (sgRNA1, sgRNA2) targeting *Pax7* exon 2 for *in vivo* deletion of *Pax7* in SCs by the CRISPR/Cas9/AAV9-dual sgRNA system. **(K)** WB showing the decreased PAX7 protein in the above isolated SCs from KD compared to Ctrl mice. The PAX7 expression level was normalized to Histone 3. Ponceau S was used as a loading control. Immunoblots are representative of two independent experiments. **(L)** SCs were isolated from Ctrl or PAX7 KD mice. Box plot depicting mean percentage of sorted QSCs in the total number of events and presented as mean ± s.d. $n = 4$ mice per group. *$P < 0.05$, two-tailed unpaired Student's *t*-test.

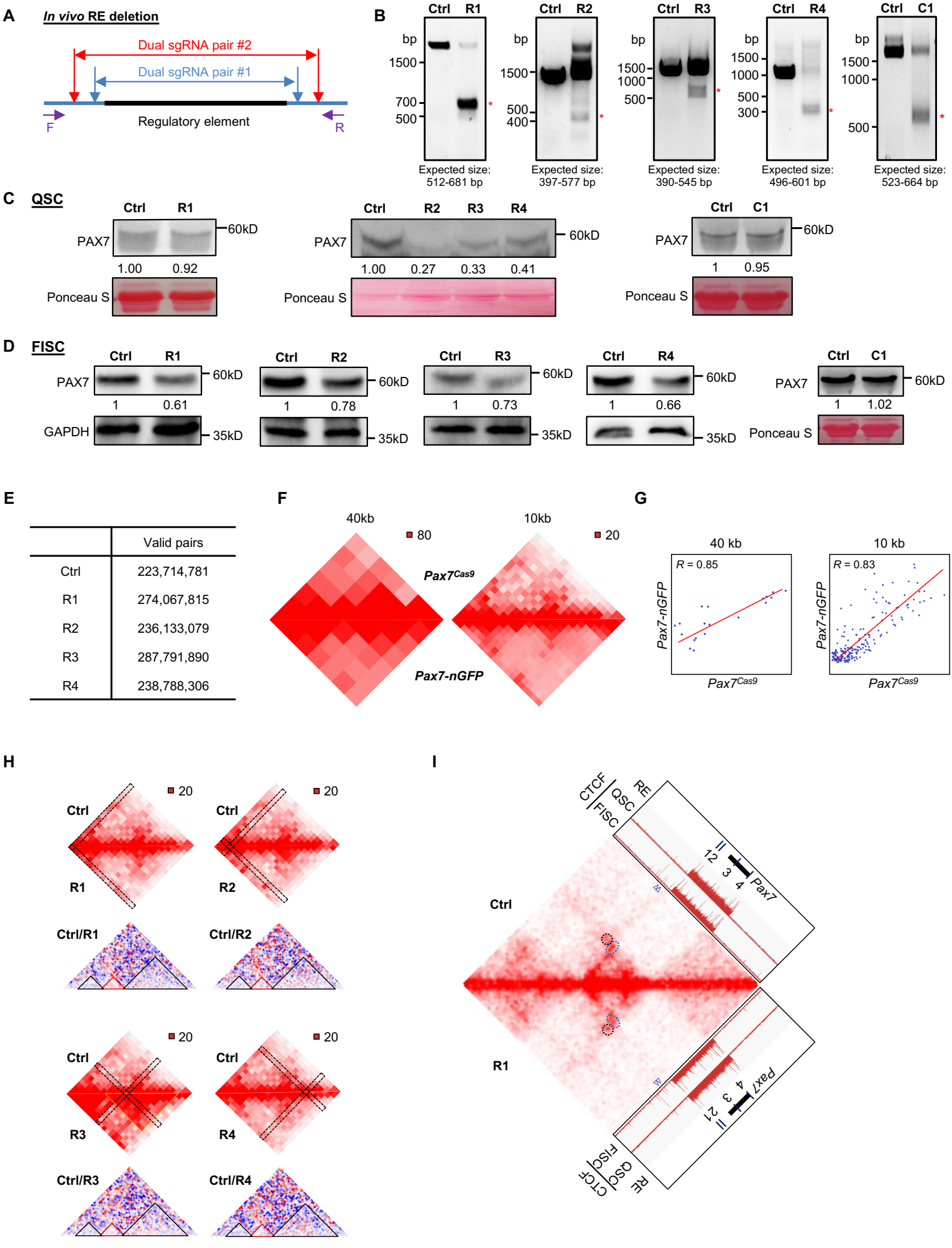
A
In vivo RE deletion
Dual sgRNA pair #2
Dual sgRNA pair #1
F
Regulatory element
R
B
Ctrl R1
Ctrl R2
Ctrl R3
Ctrl R4
Ctrl C1
bp
1500
700
500
1000
400
300
Expected size: 512-681 bp
Expected size: 397-577 bp
Expected size: 390-545 bp
Expected size: 496-601 bp
Expected size: 523-664 bp
C
QSC
PAX7
60kD
1.00 0.92
Ponceau S
1.00 0.27 0.33 0.41
1 0.95
D
FISC
GAPDH
35kD
1 0.61
1 0.78
1 0.73
1 0.66
1 1.02
E
Valid pairs
Ctrl 223,714,781
R1 274,067,815
R2 236,133,079
R3 287,791,890
R4 238,788,306
F
40kb
10kb
80
20
Pax7Cas9
Pax7-nGFP
G
40 kb
10 kb
R = 0.85
R = 0.83
Pax7-nGFP
Pax7Cas9
H
Ctrl
R1
R2
R3
R4
Ctrl/R1
Ctrl/R2
Ctrl/R3
Ctrl/R4
I
CTCF
QSC
FISC
RE
Pax7
Ctrl
R1

Figure S9. 3D regulatory interactions orchestrate *Pax7* expression dynamics in SC. (A) Schematic illustration showing the design of dual sgRNA pairs for *in vivo* deletion of individual regulatory element (RE) in SCs by the CRISPR/Cas9/AAV9-dual sgRNA system. The purple arrows (F and R) indicate PCR primers for genomic PCR analysis to assess *in vivo* deletion efficiency. **(B)** SCs were isolated from Ctrl or mutant mice and genomic PCR analysis was performed to test the cleavage efficiency. The deletion product (red asterisk) and expected size after deletion (below) are shown. **(C)** PAX7 protein level in the above QSCs was examined by Western blot. Ponceau S was used as loading control. Relative band intensity is shown. **(D)** PAX7 protein level in the above FISCs was examined by Western blot. GAPDH was used as loading control. Relative band intensity is shown. **(E)** *In situ* Hi-C was performed on QSCs isolated from Ctrl or mutant mice. The number of valid pairs generated from each sample are shown. **(F)** Comparison of contact frequencies at the TAD encompassing *Pax7* locus in QSCs from *Pax7-nGFP* or $Pax7^{Cas9}$ mice at 40 kb (left) or 10 kb (right) resolution. **(G)** Correlation of contact frequencies within the *Pax7* residing TAD between *Pax7-nGFP* and $Pax7^{Cas9}$ mice at 40 kb (Left) or 10 kb (Right) resolution. Pearson correlation coefficients (*R*) are indicated. **(H)** Comparison of contact frequencies of intra- (top) or inter- TAD (bottom) between Ctrl and RE deletion mutants. Top: The yellow triangle indicates a new sub-TAD identified in R3 QSCs. Each RE is highlighted with dotted box. Bottom: *Pax7* residing TAD is highlighted as dotted black triangle while two TADs surrounding the *Pax7* TAD are highlighted as black triangles. **(I)** Comparison of Hi-C contact maps between Ctrl and R1 QSCs. CTCF ChIP-seq in QSC and FISC are highlighted. Black circle, enhanced contact in R1 QSC; blue circle, diminished contact in R1 QSC; blue triangle, putative CTCF sites that may participate in the new loop formation in R1 QSC.

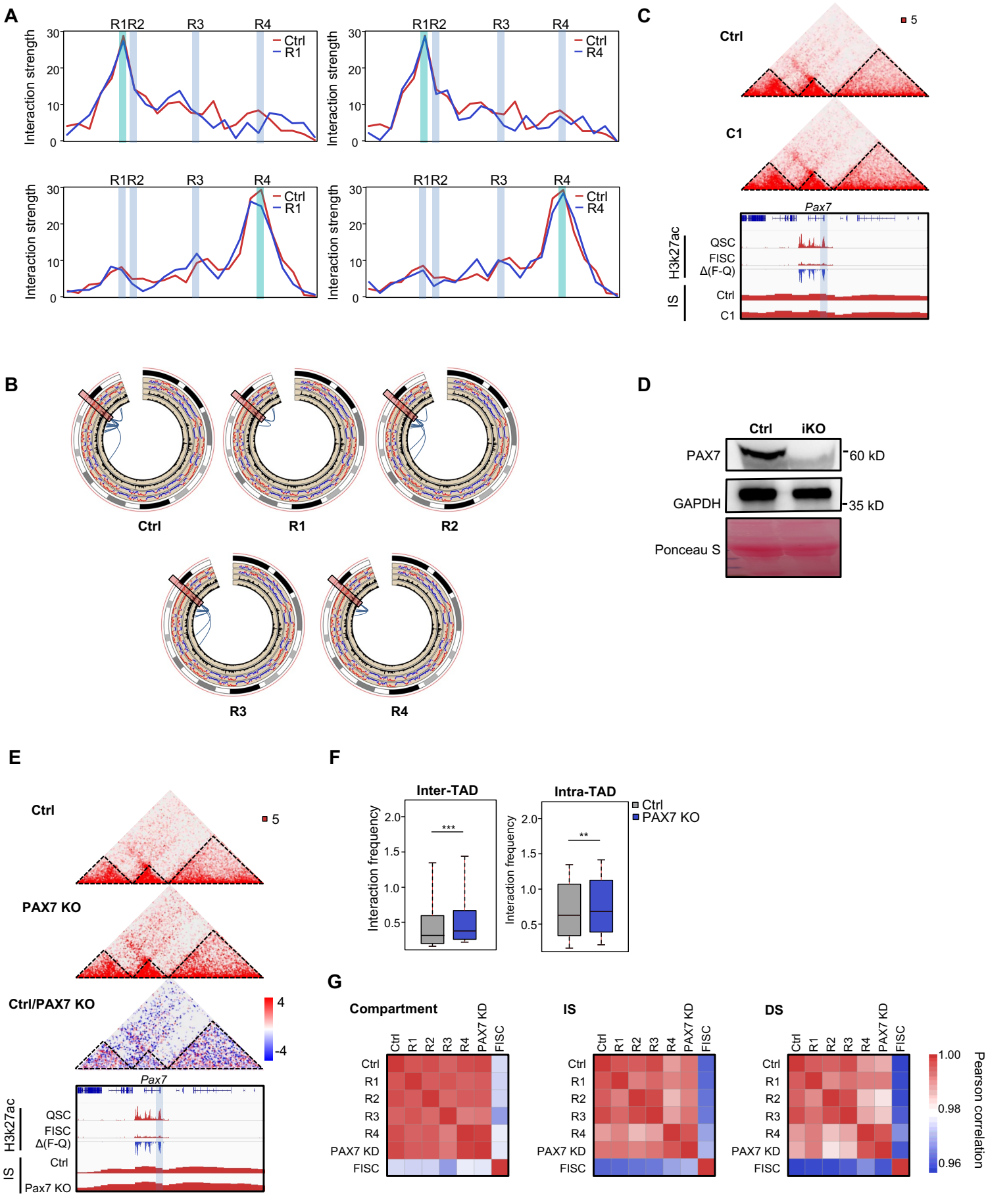
A
R1R2
R3
R4
Ctrl
R1
R4
Interaction strength
B
Ctrl
R1
R2
R3
R4
C
Ctrl
C1
5
Pax7
H3k27ac
QSC
FISC
Δ(F-Q)
IS
Ctrl
C1
D
Ctrl
iKO
PAX7
60 kD
GAPDH
35 kD
Ponceau S
E
Ctrl
PAX7 KO
Ctrl/PAX7 KO
5
4
-4
Pax7
H3k27ac
QSC
FISC
Δ(F-Q)
IS
Ctrl
Pax7 KO
F
Inter-TAD
Intra-TAD
Interaction frequency
Ctrl
PAX7 KO
***
**
G
Compartment
IS
DS
Ctrl
R1
R2
R3
R4
PAX7 KD
FISC
Pearson correlation
1.00
0.98
0.96

Figure S10. 3D regulatory interactions orchestrate *Pax7* expression dynamics in SC. (A) Virtual 4C analysis on *Pax7* locus in QSC from Ctrl or RE mutant mice. **(B)** Circos diagrams showing the intra-chromosome interaction between the loci in *Pax7* TAD (red box) and other loci in Ctrl and mutant QSCs. **(C)** Hi-C contact maps (10-kb resolution) showing *Pax7* TAD organization in C1 group in comparison with Ctrl group. **(D)** WB showing the deletion of PAX7 protein in FISCs collected from *Pax7* iKO vs. Ctrl mice. GAPDH and Ponceau S were used as loading controls. Immunoblots are representative of two independent experiments. **(E)** Hi-C contact maps (10-kb resolution) showing *Pax7* TAD reorganization in the *Pax7* iKO QSC in comparison with Ctrl. **(F)** Boxplots showing inter- (between the *Pax7* TAD and other *cis*-interacting TADs) or intra-TAD (within *Pax7* TAD) interactions. $^{**}P < 0.001$, $^{***}P < 0.0001$, Wilcoxon signed-rank test. **(G)** Heatmap showing the Pearson correlation among Ctrl QSC, RE deletion QSC (R1, R2, R3, R4), *Pax7 in vivo* knockdown QSC and FISC, based on the PC1 values (100 kb bins), IS values (40 kb bins) and DS (40 kb bins).

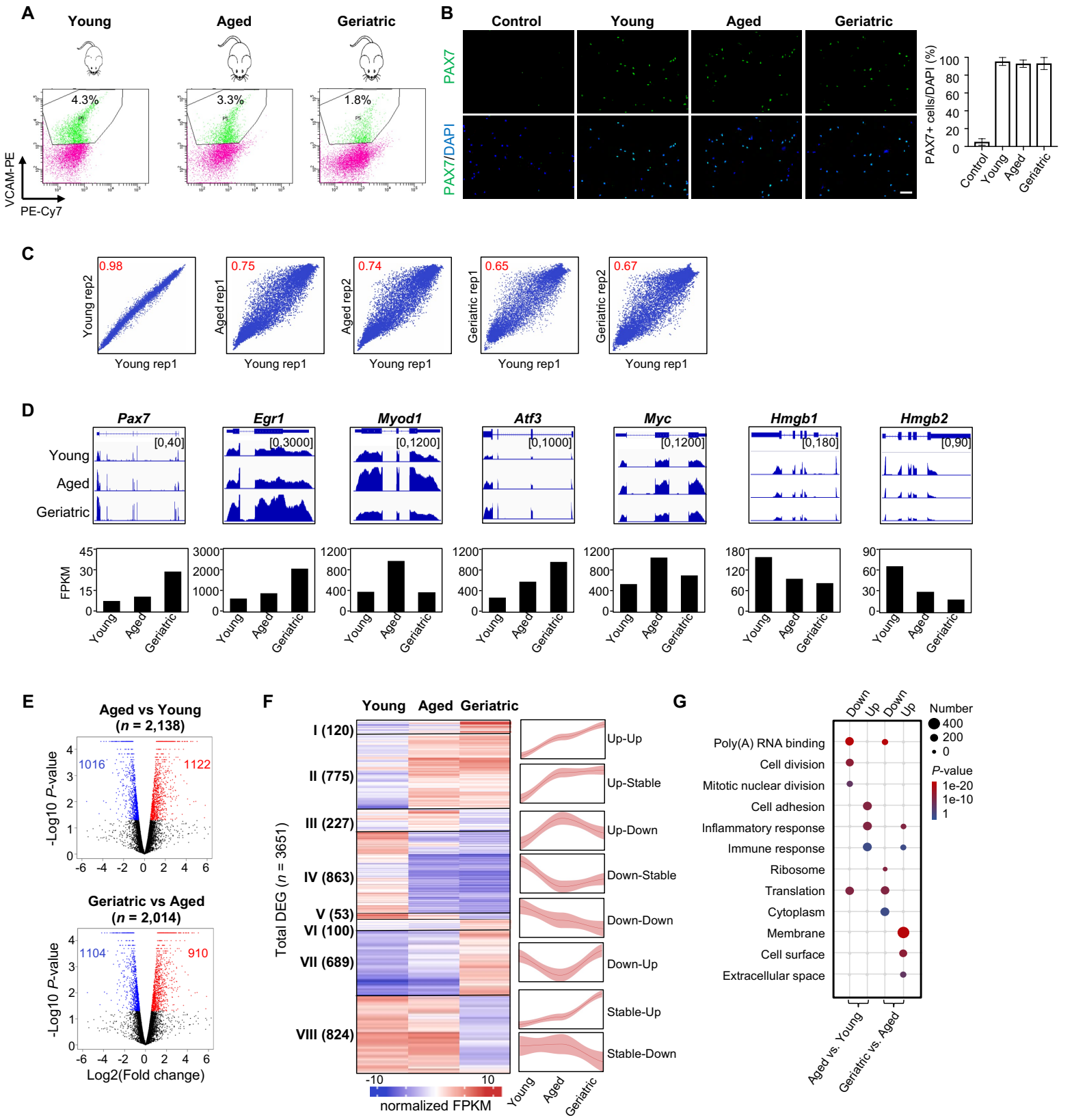
A
Young
Aged
Geriatric
4.3%
3.3%
1.8%
VCAM-PE
PE-Cy7
B
Control
Young
Aged
Geriatric
PAX7
PAX7/DAPI
PAX7+ cells/DAPI (%)
C
0.98
0.75
0.74
0.65
0.67
Young rep2
Young rep1
Aged rep1
Aged rep2
Geriatric rep1
Geriatric rep2
D
Pax7
Egr1
Myod1
Atf3
Myc
Hmgb1
Hmgb2
Young
Aged
Geriatric
FPKM
E
Aged vs Young
(n = 2,138)
1016
1122
Geriatric vs Aged
(n = 2,014)
1104
910
-Log10 P-value
Log2(Fold change)
F
Young Aged Geriatric
I (120)
II (775)
III (227)
IV (863)
V (53)
VI (100)
VII (689)
VIII (824)
Total DEG (n = 3651)
normalized FPKM
Up-Up
Up-Stable
Up-Down
Down-Stable
Down-Down
Down-Up
Stable-Up
Stable-Down
G
Down
Up
Down
Up
Number
P-value
Poly(A) RNA binding
Cell division
Mitotic nuclear division
Cell adhesion
Inflammatory response
Immune response
Ribosome
Translation
Cytoplasm
Membrane
Cell surface
Extracellular space
Aged vs. Young
Geriatric vs. Aged

Figure S11. Dynamics of transcriptome during mouse SC aging. (A) VCAM+ FISCs were collected from young (2 months), aged (23-24 months) and geriatric (28-32 months) C57BL/6J mice. FACS profiles are shown and the gates indicate the population of FISCs isolated for following analysis. Values on the plots indicate mean percentage of sorted FISCs in the total number of events. (**B)** Left: PAX7 IF staining was performed on the above collected cells. Scale bar, 50 μm. (right) the percentages of PAX7+ cells in FISCs are plotted. Control, young FISCs stained with secondary antibody only, depicting the background signal. n = 10 fields. (**C)** Scatter plots showing RNA expression (FPKM) changes in aged or geriatric relative to young FISC expression. Pearson correlation coefficient (R) is indicated in red. (**D)** (top) Genome browser view of *Pax7*, *Egr1*, *Myod1*, *Atf3*, *Myc*, *Hmgb1* and *Hmgb2* gene expression measured by RNA-seq; bottom: bar graph showing the RPKM values of the above genes. (**E)** Volcano plot of differentially expressed genes (DEGs) in Aged vs. Young (top) and Geriatric vs. Aged (bottom) FISCs. The blue and red dots lying in left and right represent significantly down- and up-regulated genes, respectively (P-value ≤ 0.05, linear fold change ≤ -2 or ≥ 2). Number of down- and up-regulated genes is also indicated. **(F)** k-means clustering (k = 8) of DEG profiles showing the kinetics for 8 clusters. Line graphs on the right depict kinetics of gene expression changes. Lines denote the mean values, while the shaded ribbons represent the 95% confidence interval (CI). (**G)** Bubble plot showing the enriched GO terms of genes associated with the indicated category. The bubble size represents the number of genes enriched in each term; the bubble color represents the enrichment significance.

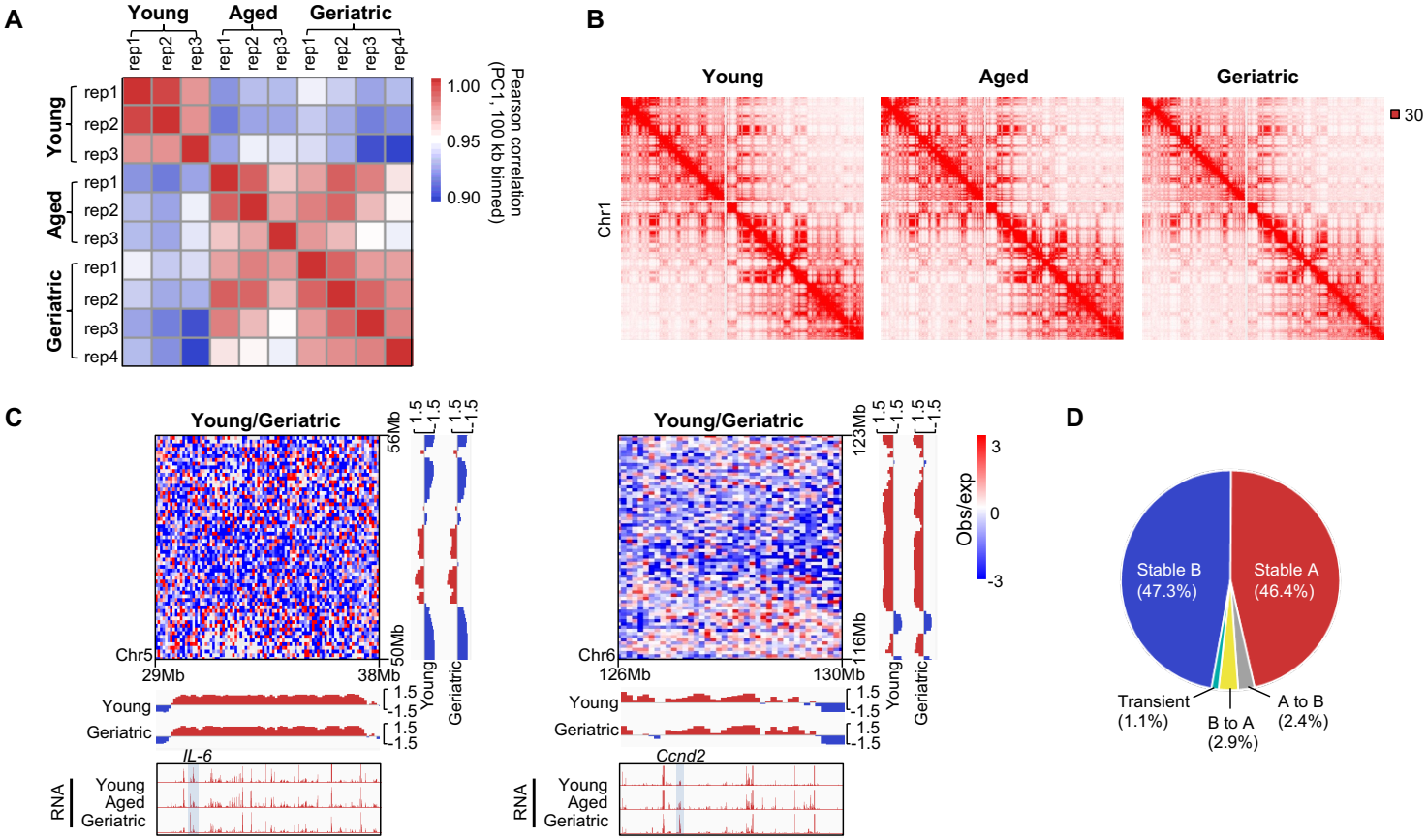
A
Young
Aged
Geriatric
rep1
rep2
rep3
rep4
Pearson correlation (PC1, 100 kb binned)
1.00
0.95
0.90
B
Young
Aged
Geriatric
Chr1
30
C
Young/Geriatric
Chr5
29Mb
38Mb
56Mb
50Mb
Young
Geriatric
IL-6
RNA
Young
Aged
Geriatric
Young/Geriatric
Chr6
126Mb
130Mb
123Mb
116Mb
Ccnd2
Obs/exp
3
0
-3
D
Stable B (47.3%)
Stable A (46.4%)
Transient (1.1%)
B to A (2.9%)
A to B (2.4%)
E
Chr11:62.85-63.05 Mb
Pmp22
Chr11:81.79-81.92 Mb
Ccl2 Ccl7Ccl11
Ccl12
Chr11:66.98-67.10 Mb
Myh2
Myh1
Myh4
Myh8
PC1
A/B (-0.5,0.5)
RNA-seq (0,200)
RNA-seq (0,400)

Figure S12. Global reorganization of genome compartmentalization during mouse SC aging. (A) Heatmap showing the Pearson correlation among replicates of Hi-C libraries, based on the PC1 values (100 kb bins). **(B)** Observed contact matrices for Chr1 at 500-kb resolution during SC aging. The scale is adjusted to account for the total coverage on Chr1 at each stage. **(C)** (left) Differential heatmap on chromosome 6 showing increased A-A interactions in Geriatric vs. Young FISC, accompanied with an increase in *Il-6* mRNA expression. (right) Differential heatmap on chromosome 15 showing increased A-A interactions in Geriatric vs. Young FISC, accompanied with increase in *Ccnd2* mRNA expression. PC1 signals at each stage are displayed on the bottom of the heatmap. **(D)** Pie chart depicting fraction of the genome with or without compartment switching during SC aging. **(E)** Genome-browser view of *Pmp22* (left), *Ccl2-Ccl7-Ccl11* (middle) and *Myh1-Myh4* (right) loci. PC1 and RNA-seq at each stage are shown. Green shade indicates compartment switching.

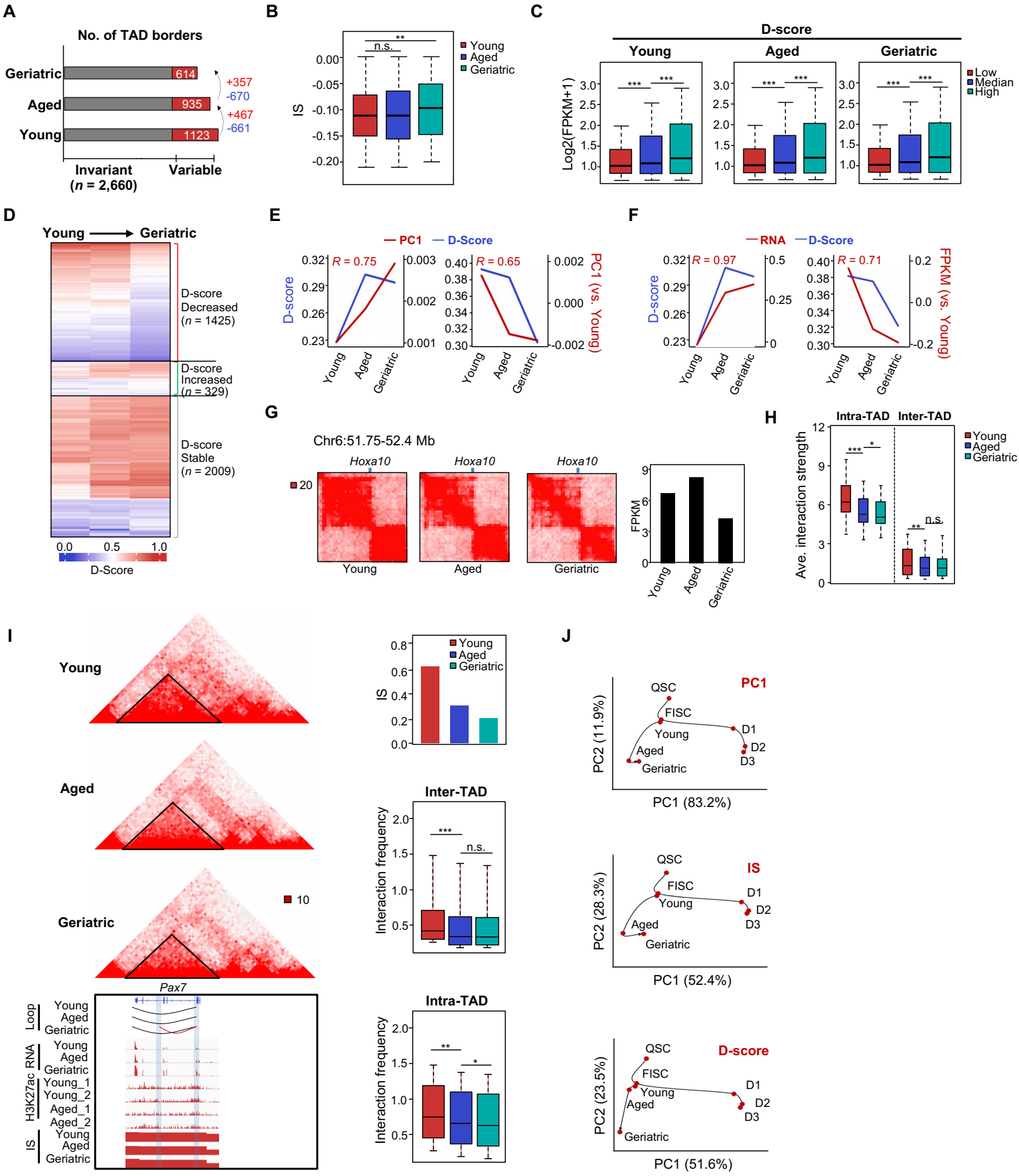
A
No. of TAD borders
Geriatric
Aged
Young
614
935
1123
+357
-670
+467
-661
Invariant
(n = 2,660)
Variable
B
IS
n.s.
**
Young
Aged
Geriatric
C
D-score
Young
Aged
Geriatric
Log2(FPKM+1)
***
Low
Median
High
D
Young → Geriatric
D-score
Decreased
(n = 1425)
D-score
Increased
(n = 329)
D-score
Stable
(n = 2009)
0.0
0.5
1.0
D-Score
E
PC1
D-Score
R = 0.75
R = 0.65
D-score
PC1 (vs. Young)
F
RNA
D-Score
R = 0.97
R = 0.71
FPKM (vs. Young)
G
Chr6:51.75-52.4 Mb
Hoxa10
20
Young
Aged
Geriatric
FPKM
H
Intra-TAD
Inter-TAD
Ave. interaction strength
n.s.
I
Young
Aged
Geriatric
10
Pax7
Loop
RNA
H3K27ac
Young_1
Young_2
Aged_1
Aged_2
IS
Inter-TAD
Intra-TAD
Interaction frequency
J
PC1
PC2 (11.9%)
PC1 (83.2%)
QSC
FISC
Young
Aged
Geriatric
D1
D2
D3
IS
PC2 (28.3%)
PC1 (52.4%)
D-score
PC2 (23.5%)
PC1 (51.6%)

Figure S13. Multiscale analysis of 3D genome during mouse SC aging. (A) The number of TAD borders identified per time point. Invariant borders are present at all stages while variable borders are lost or acquired in between two adjacent stages. **(B)** Box plot depicting the IS of TAD borders at each stage. **(C)** Boxplots depicting expression of genes in TADs with a low (0, 0.3), average (0.3, 0.6) or high (0.6, 0.9) relative domain score (D-score). **(D)** Hierarchical clustering showing the kinetics for groups with increased ($n = 329$), decreased ($n = 1{,}425$), or stable ($n = 2{,}009$) D-scores during SC aging. **(E-F)** Average D-score and PC1 kinetics **(E)** or gene expression **(F)** analysis for clusters of TADs that were gained or lost in Geriatric vs. Young. Pearson correlation coefficients (R) are indicated. **(G)** (left) Illustration of *in situ* Hi-C contact maps (40-kb resolution) on the *Hoxa10* locus. Bar graph showing the FPKM kinetics of *Hoxa10* expression during SC aging. **(H)** Contact enrichment of intra- and inter-TADs during SC aging. Data are represented as boxplots based on the intra- and inter-TAD values per TAD. **(I)** Hi-C contact maps depicting *Pax7* TAD reorganization during SC aging. Genome-browser view of chromatin loops, *Pax7* RNA expression, H3K27ac signals in Young and Aged FISCs, and IS around *Pax7* locus during SC aging. Bar plot showing the IS values of the above borders. Boxplots showing inter- or intra-TAD interactions. **(J)** PCA analysis of PC1 values, IS, and D-score during SC lineage progression and SC aging. Black arrows denote the hypothetical trajectory. Data in B, C and I are presented in boxplots. *$P <$ 0.01, **$P < 0.001$, ***$P < 0.0001$, Wilcoxon signed-rank test.

Fig. 3E

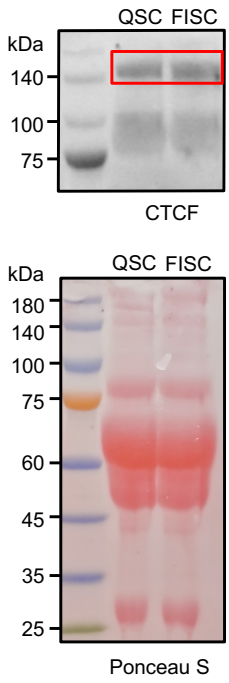

Fig. S8B

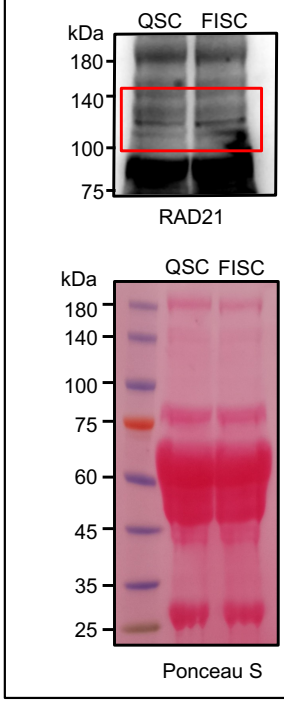

Fig. S8K

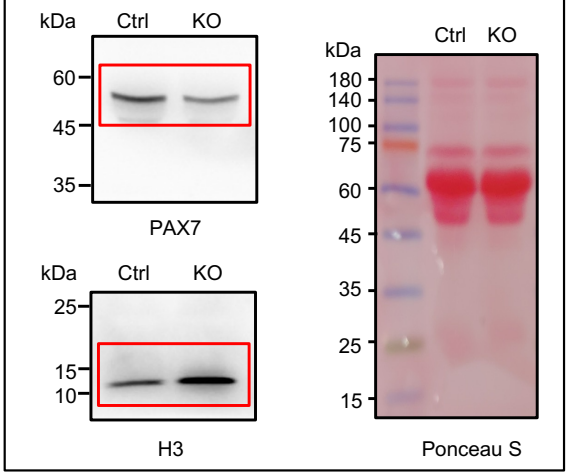

Fig. S9B

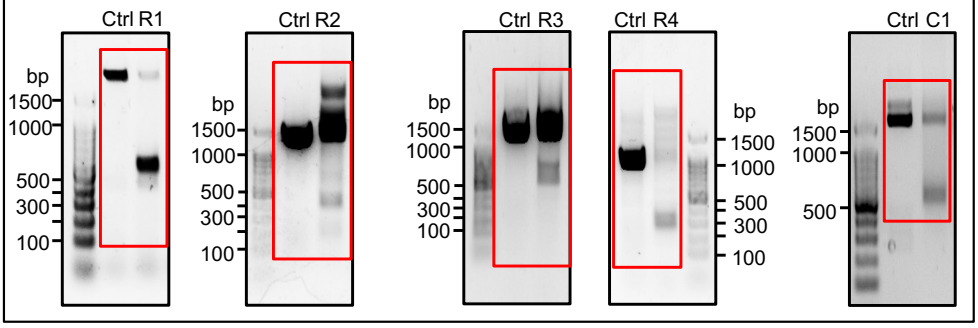

Figure S14. Source data for gel images and immunoblots relating to Fig. 3E, S8B, S8K and S9B.

Fig. S9C

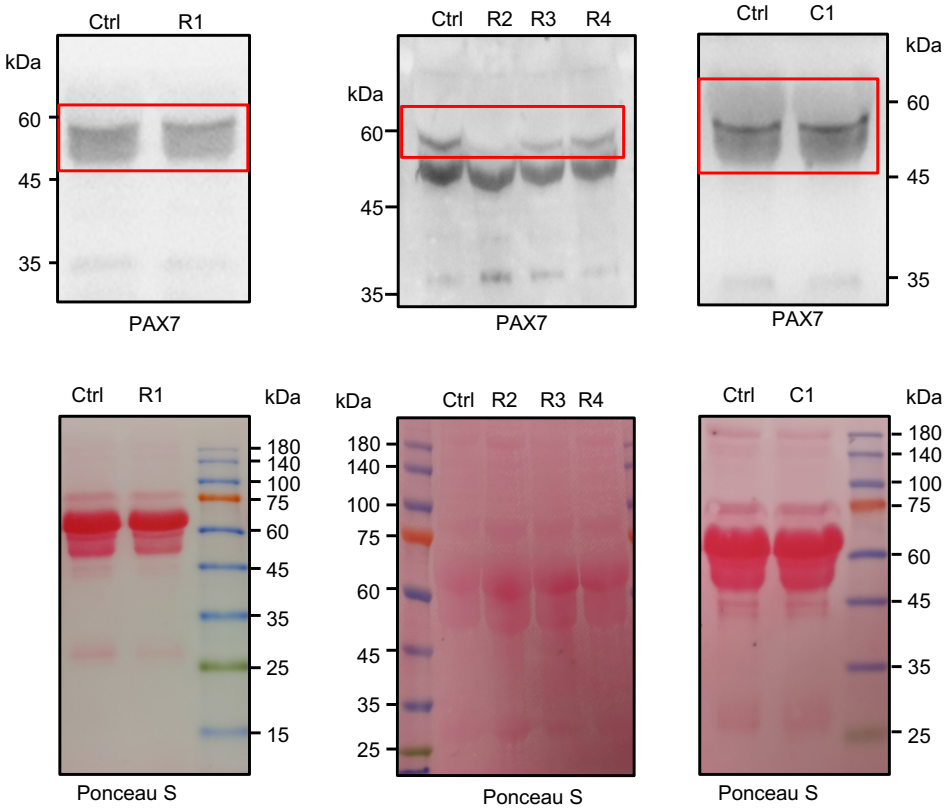

Fig. S9D

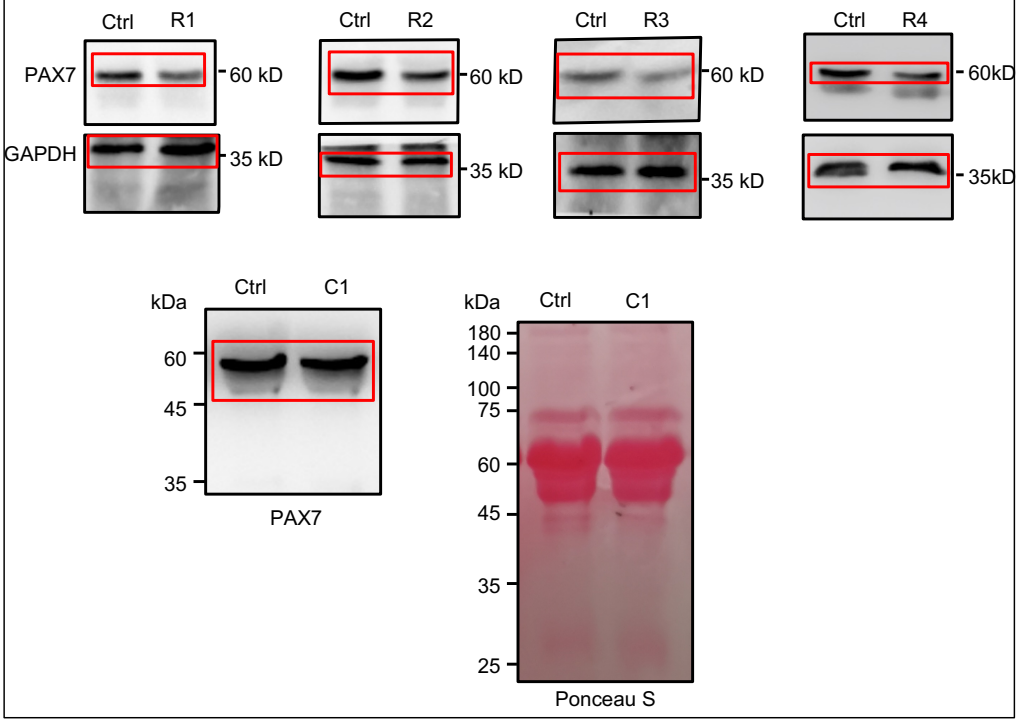

Fig. S10C

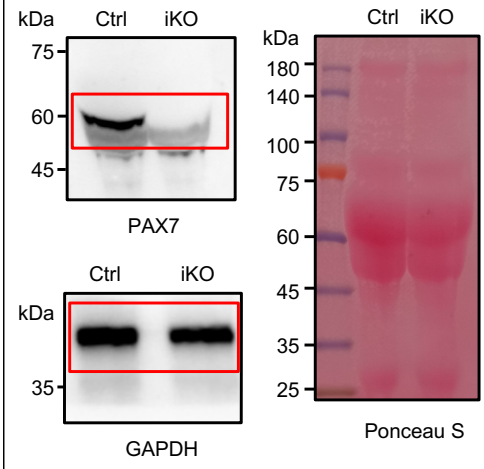

Figure S15. Source data for immunoblots relating to Fig. S9C, S9D and S10C.

Table S1. (separate file)
Basic statistics of *in-situ* Hi-C data.

Table S2. (separate file)
Compartment analysis during SC lineage progression.

Table S3. (separate file)
RNA-seq analysis during SC lineage progression.

Table S4. (separate file)
TAD analysis during SC lineage progression.

Table S5. (separate file)
TAD cluster analysis during SC lineage progression.

Table S6. (separate file)
Loop analysis from QSC to FISC.

Table S7. (separate file)
Pax7 KO analysis in QSC.

Table S8. (separate file)
RNA-seq analysis in aging SCs.

Table S9. (separate file)
Compartment analysis during SC aging.

Table S10. (separate file)
TAD and loop analysis during SC aging.

Table S11. (separate file)
Sequences of oligos used in the study.

Table S12. (separate file)
Summary of all public datasets used in the study.